

# Chiral Protein Scissors Activated by Light: Recognition and Protein Photocleavage by a New Pyrenyl Probe

Apinya Buranaprapuk,<sup>\*,†,‡</sup> Yaowaluk Malaikaew,<sup>‡</sup> Jisnusun Svasti,<sup>§</sup> and Challa V. Kumar<sup>\*,†</sup>

Department of Chemistry, University of Connecticut, U-3060, 55 N. Eagleville Road, Storrs, Connecticut 06269-3060, Department of Chemistry, Faculty of Science, Srinakharinwirot University, Sukhumvit 23, Bangkok 10110, Thailand, and Department of Biochemistry, Faculty of Science, Mahidol University, Rama VI Road, Bangkok 10400, Thailand

Received: April 1, 2008; Revised Manuscript Received: May 9, 2008

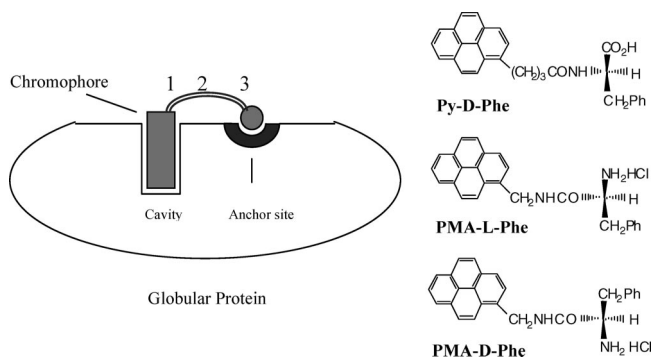
Strong chiral discrimination and site-selective photocleavage of two model proteins, lysozyme and bovine serum albumin (BSA), by new pyrenyl probes are reported here. The enantiomeric pyrenyl probes D-phenylalanine-1(1-pyrene)methylamide (PMA-D-Phe) and L-phenylalanine-1(1-pyrene)methylamide (PMA-L-Phe) were synthesized by coupling the carboxyl function of D-phenylalanine or L-phenylalanine with the amino group of 1(1-pyrene)methylamine. Binding affinities of the two enantiomers with the proteins were quantitated in absorption titrations. BSA indicated 10-fold selectivity for PMA-D-Phe, and the binding constants for the L- and D-enantiomers were  $3.8 \times 10^5$  and  $4.0 \times 10^6 \text{ M}^{-1}$ , respectively. Lysozyme, similarly, indicated a 6-fold preference for PMA-D-Phe with binding constants of  $3.3 \times 10^5$  and  $2.0 \times 10^6 \text{ M}^{-1}$  for the L- and D-isomers, respectively. Such strong chiral discrimination illustrates the key role of the chiral center of the probe (Phe) in the binding interactions. The enantiomers were tested to examine how the chiral discrimination for their binding influences reactivity toward protein photocleavage. Irradiation of the probe–protein complexes, at 342 nm in the presence of hexammine cobalt(III) chloride, resulted in the cleavage of the protein backbone. Photocleavage did not proceed in the dark or in the absence of the pyrenyl probes. Both enantiomers indicated low reactivity with BSA (<5% yield), while large photocleavage yields (~57%) have been noted with lysozyme. This lysozyme photocleavage yield is a significant improvement over previous reports. However, both enantiomers cleaved lysozyme at the same location between Trp108–Val109, despite the strong chiral selectivity for binding. H-atom abstraction from Trp 108, accessible from the active site cleft, could initiate the observed peptide bond cleavage.

## Introduction

The design of small molecules that are capable of chiral discrimination of specific sites on proteins as well as cleaving the peptide backbone on demand, under thermal or photochemical conditions, is quite challenging. To date, only a handful of molecules have been known to have this ability, and expanding this repertoire is very important.<sup>1,2</sup> This is because the design of such reagents should include (1) appropriate recognition elements for binding to the target site with high affinity and (2) reactive groups which can be activated to produce the desired cleavage chemistry with high selectivity. One advantage of using light to induce protein cleavage is that the reaction can be initiated, sustained, or terminated conveniently, reactive intermediates can be followed in time-resolved studies, and light can be a noninvasive, green component of the reaction mixture.

The current design consists of a modular approach with three distinct units providing significant control over the properties of the probe (Chart 1).<sup>3,4</sup> A hydrophobic unit is used for binding at a suitable hydrophobic cleft on the protein, while a polar group anchors the probe by interacting with complementary functions on the surface of the protein. A short linker of suitable length, and flexibility, spans these two units.<sup>5</sup> For example, the

**CHART 1:** (left) Schematic of the Modular Design of a Probe, Which Is Capable of Making a Two-Point Contact on the Surface of a Globular Protein;<sup>a</sup> (right) Structures of D-Phenylalanine-4(1-pyrene)butyramide (Py-D-Phe), L-Phenylalanine-1(1-pyrene)methylamide (PMA-L-Phe), and D-Phenylalanine-1(1-pyrene)methylamide (PMA-D-Phe)



<sup>a</sup> While the chromophore (1) binds in a hydrophobic cavity on the surface, the polar group (3) anchors the probe, and the linker (2) connects the two units in a suitable manner.

pyrenyl chromophore (hydrophobic unit) is linked to the amino terminus of L-phenylalanine by a short chain (Py-L-Phe).<sup>1</sup> By varying the modules of this design, a number of chiral probes with significant binding affinities for proteins were obtained.<sup>6–9</sup> A key feature of our photochemical approach has been that the

\* Corresponding authors. Phone: 662-649-5000 (ext. 8452) (A.B.); 860-486-3213 (C.V.K.). Fax: 662-259-2097 (A.B.); 860-486-2981 (C.V.K.). E-mail: apinyac@swu.ac.th (A.B.); Challa.Kumar@uconn.edu (C.V.K.).

<sup>†</sup> University of Connecticut.

<sup>‡</sup> Srinakharinwirot University.

<sup>§</sup> Mahidol University.

newly formed amino terminus of the peptide is amenable to amino acid sequencing. Consequently, the photocleavage sites were mapped successfully in sequencing studies,<sup>10</sup> and similar reagents have been used to study protein orientation at solid surfaces.<sup>11</sup>

The choice of the pyrenyl chromophore in the modular design is justified. It has (1) a long-lived, high energy singlet excited state,<sup>12</sup> which can be used to sensitize chemical reactions, (2) strong absorption bands in the near-UV region,<sup>13</sup> which are sensitive to the environment of the chromophore, and (3) strong fluorescence bands in the visible region, which are useful to monitor binding to proteins,<sup>14</sup> and (4) the pyrene nucleus is amenable to substitution for the synthesis of a number of derivatives.<sup>15</sup>

The modular approach provided unique opportunities to test the roles of specific structural features of the probe in the binding as well as protein photocleavage chemistry. Understanding the contributions of these modules to the properties of the probe will be useful for the rational design of better reagents. For example, use of Tyr or Trp residues in the linker completely inhibited the protein photocleavage, while replacement by His restored the photoreactivity.<sup>6</sup> Increasing the distance between the pyrenyl chromophore and the carboxy terminus residue, by inserting increasing numbers of Gly residues in the linker, allowed the control of the protein cleavage along the peptide.<sup>5</sup> Thus, the linker has an important role in the binding and photocleavage properties of the above probes.

The protein scissors of this family, thus far, contained a free carboxyl terminus, and the corresponding ester derivatives indicated considerably lower affinities and photocleavage yields.<sup>10</sup> The effect of reversing the direction of the peptide linkages in the linker and replacing the carboxyl function by an amino group was reported, recently.<sup>9</sup> The cationic probe PMA-L-Phe (Chart 1) differs from Py-Phe in terms of its charge, the end group, the direction of the peptide bond in the linker, and the linker length. PMA-Phe also demonstrated strong binding to proteins as well as excellent protein photocleavage properties.

The goal of the current studies is to examine if the decreased distance of separation between the asymmetric center (Phe) and the pyrenyl chromophore in PMA-Phe would enhance the chiral recognition of PMA-Phe enantiomers. The three-atom linker of PMA-Phe is shorter than the five-atom linker of Py-Phe, and this is expected to increase the chiral discrimination at the protein binding site. The PMA-Phe enantiomers showed significant chiral discrimination with two proteins, but it is interesting to note that the chiral selectivity observed here is opposite to that of Py-Phe enantiomers. These probes are among the very few non-natural molecules, which indicated strong chiral recognition with proteins. The details of our investigations are presented below.

## Materials and Methods

Lysozyme (mol. wt. = 14 300) and BSA (mol. wt. = 66 267) were purchased from Sigma Chemical Co. (St. Louis, MO), and the protein solutions have been prepared by dissolving appropriate amounts of the protein in 50 mM Tris-HCl buffer, pH 7.0 (Tris buffer). All solutions were prepared fresh and used on the same day. The absorption spectra were recorded on a Hewlett-Packard model 8453 diode-array spectrophotometer. Calibration graphs were constructed using Beer's law (1 cm path length), and probe concentrations have been restricted to the linear region of the calibration graph. The molar extinction coefficient of 46 000 M<sup>-1</sup> cm<sup>-1</sup> in Tris buffer at 342 nm was

obtained for both PMA-L-Phe and PMA-D-Phe. The absorption spectral data are used to construct binding isotherms using the Scatchard equation (eq 1).<sup>16</sup> In eq 1, the concentration of the free chromophore ( $C_f$ ) is related to the binding constant ( $K_b$ ), the binding site size ( $n$ ), and the binding density ( $r$ ).

$$1/C_f = K_b(n/r - 1) \quad (1)$$

The fluorescence spectra were recorded on a Jasco FP-6200 spectrofluorometer. The spectral titrations were performed by varying the protein concentration, while keeping the probe concentration constant, in air-saturated solutions. In fluorescence experiments, the pyrenyl probe was excited at a wavelength where there is no change in its absorption as a function of protein concentration (isosbestic point, 344 nm). The fluorescence intensity was monitored at 377 or 378 nm, as a function of protein concentration.

**Synthesis of the Probe.** PMA-D-Phe was synthesized by coupling 4-(1-pyrene)methylamine (1 g) with *N*-*t*-Boc-D-phenylalanine (1 g) using dicyclohexylcarbodiimide (DCC) (1.2 g) by following a procedure similar to that used for the synthesis of Py-L-Phe.<sup>2</sup> The *t*-Boc group was removed by acid hydrolysis (50% TFA/CH<sub>2</sub>Cl<sub>2</sub> + 5% triisopropylsilane). The synthesis of PMA-L-Phe was performed in the same way as that of PMA-D-Phe except that *N*-*t*-Boc-L-phenylalanine was used instead of *N*-*t*-Boc-D-phenylalanine. Both products were identified by UV-vis, fluorescence, circular dichroism, NMR, and mass spectral data. For PMA-D-Phe (70% yield): <sup>1</sup>H NMR (400 MHz, *d*<sub>6</sub>-DMSO): 7.9–8.2 ppm (9H), 7.1–7.2 ppm (5H), 5.0–5.2 ppm (2H), 4.0 ppm (1H), 3.7 ppm (1H), 2.1 ppm (2H), 1.7 ppm (2H). MS data (FAB): *m/e* 758.4 (2MH<sup>+</sup>), mp: 120 °C. For PMA-L-Phe (80% yield): <sup>1</sup>H NMR (400 MHz, *d*<sub>6</sub>-DMSO): 7.9–8.3 ppm (9H), 7.2–7.3 ppm (5H), 5.2 ppm (2H), 4.0 ppm (1H), 3.7 ppm (1H), 2.0 ppm (2H), 1.7 ppm (2H). MS data (FAB): *m/e* 757.9 (2MH<sup>+</sup>), mp: 120 °C.

**Photochemical Protein Cleavage.** The protein photocleavage was carried out in 50 mM Tris-HCl buffer, pH 7.0. The protein solution (15 μM), containing PMA-D-Phe (or PMA-L-Phe, 15 μM) and Co(NH<sub>3</sub>)<sub>6</sub>Cl<sub>3</sub> (CoHA, 1 mM) (total volume 100 μL), was irradiated at 342 nm using a 150 W xenon lamp attached to a PTI model A1010 monochromator. A UV cutoff filter (WG-345; 78%T at 342 nm) was used to remove stray UV light. Dark control samples were prepared under the same conditions, as described above, except that the solutions were protected from light. Protein samples were evaporated under vacuum using a SpeedVac (ThermoQuest, model ISS 110) for gel electrophoresis experiments.

**Sodium Dodecylsulfate-Polyacrylamide Gel Electrophoresis (SDS-PAGE).** The irradiated samples (100 μL) were dried in a SpeedVac, and the sample was dissolved in the loading buffer (24 μL) containing SDS (7% w/v), glycerol (4% w/v), Tris (50 mM, pH 6.8), mercaptoethanol (2% v/v), and Bromophenol blue (0.01% w/v). The protein solutions (8 μL) were denatured by heating at 100 °C for 3 min. The polyacrylamide gel was prepared by following a literature procedure.<sup>17</sup> To separate the reaction mixture containing BSA, 8% polyacrylamide (separating) gel was used, while the lysozyme reaction mixture was separated using a 12% polyacrylamide gel. The gel was electrophoresed by applying 60 V until the dye passed into the separating gel and then the voltage increased to 110 V. The gels were run for 2 h, stained with Coomassie Blue, and destained in acetic acid solution (10%). Bands in the gels were quantified using NIHimage software (v 1.6) as described earlier,<sup>10</sup> and the yields were calculated with respect to the unreacted protein bands. In the quenching studies, the photo-

reactions were performed as above but various concentrations (0–50 mM) of ethanolamine were added to the probe/protein mixtures prior to irradiation. A calibration graph of the standard proteins was constructed to estimate the molecular masses of the photofragments.

**Western Transfer of Photofragments.** The protein fragments separated on 12% SDS-polyacrylamide gel were transferred to PVDF membrane by applying a current of 60 mA for 1.5 h by the semidry system (BIORAD) in CAPS (3-(cyclohexylamino)-1-propanesulfonic acid) buffer, pH 10.5. The transferred protein bands were stained with Coomassie brilliant blue (0.1% Coomassie brilliant blue R-250 in 40% methanol and 1% acetic acid). The desired bands were cut and submitted for N-terminal sequencing analysis (Midwest Analytical, Inc., St. Louis, MO). Chemical sequencing was performed on an automated protein sequencer. At least five cycles were performed to identify the N-terminus.

## Results and Discussion

Chiral pyrenyl probes containing a hydrophobic unit, a polar function, and a short linker are investigated here for their binding and protein photocleavage properties. The short linker of PMA-Phe is expected to position the pyrenyl chromophore closer to the asymmetric center, and this may enhance discrimination by the probe. We investigated how the proximity between the polar and hydrophobic units controls the chiral selectivity of the pyrenyl probe. Our results are as follows.

**Absorption Titrations.** The electronic absorption spectral features of the pyrenyl chromophore are sensitive to its microenvironment,<sup>18</sup> and protein binding produces perceptible changes in its absorption spectral characteristics. Addition of a concentrated solution of BSA (10  $\mu$ M) to a solution of PMA-D-Phe (2  $\mu$ M) resulted in gradual red shifts of the absorption peak positions of the pyrenyl chromophore (Figure 1A). The spectra have been corrected for small decreases in the intensity when the volume increased during the titration. The absorbance spectra underwent smooth changes with a crossing point at  $\sim$ 344 nm, as the protein solution was titrated (0–12  $\mu$ M BSA). Note that there is no clear isosbestic point, the wavelength at which the absorbance is independent of the protein concentration, and this indicates the conversion of one form of the chromophore (free) to two or more bound species. For example, the spectrum recorded at 4.0  $\mu$ M BSA is distinct from the first or the last spectrum, and several spectroscopically similar chromophores are present in the system. The red shift noted at high concentrations of BSA clearly indicates the decrease of the HOMO–LUMO gap. Such red shifts are noted when the pyrene chromophore is exposed to hydrophobic solvents.<sup>1</sup> Similar red shifts (2 nm) are also observed with PMA-L-Phe bound to BSA, under the same pH and ionic strength conditions (Table 1). These observations suggest the intriguing possibility that the two probes may reside at the same site on BSA.

The absorption spectra shown in Figure 1A are further analyzed by plotting the decrease in absorbance at 342 nm and growth at 345 nm, as a function of BSA concentration (inset in Figure 1A). The absorption changes at the two wavelengths complement each other, and the binding saturates at high concentrations (10  $\mu$ M) of the protein.

In contrast to the significant spectral changes observed with BSA, only minor changes were noted when PMA-D-Phe was titrated with lysozyme. For example, the absorption spectra of PMA-D-Phe (2.2  $\mu$ M) indicated only minor changes in the presence of increasing concentrations of lysozyme (0–10  $\mu$ M, Figure 1B). These spectra were also corrected for small changes

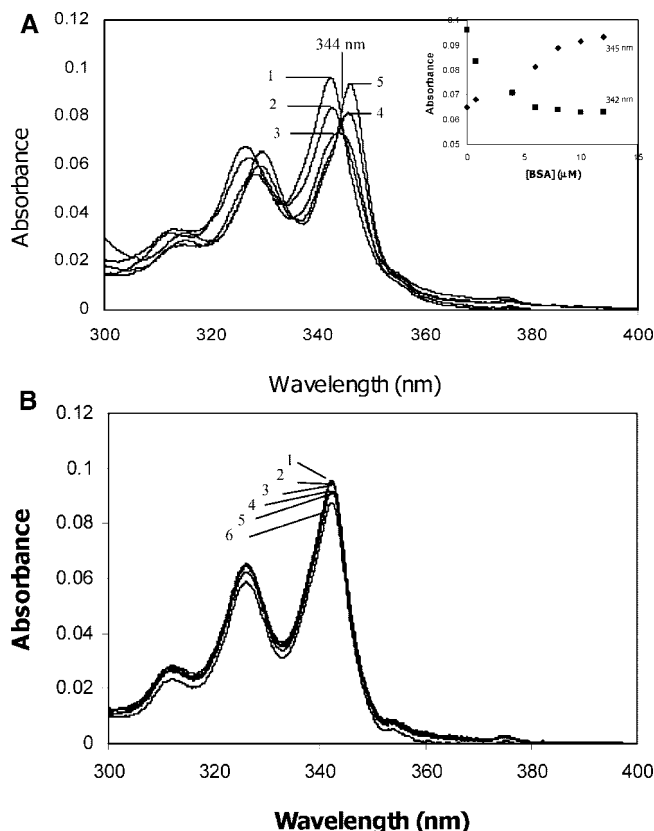


**Figure 1.** (A) Absorption spectra of PMA-D-Phe (2  $\mu$ M) in the presence of increasing concentrations of BSA: (1) 0  $\mu$ M, (2) 0.80  $\mu$ M, (3) 4.0  $\mu$ M, (4) 8.0  $\mu$ M, and (5) 12.0  $\mu$ M. The path length is 1 cm. The inset shows a plot of absorbance at 345 or 342 nm vs BSA concentration. (B) Absorption spectra of PMA-D-Phe (2.2  $\mu$ M) recorded in the presence of increasing concentrations of lysozyme: (1) 0  $\mu$ M, (2) 2  $\mu$ M, (3) 4  $\mu$ M, (4) 6  $\mu$ M, (5) 8  $\mu$ M, and (6) 10  $\mu$ M.

**TABLE 1: Binding Properties of PMA-D-Phe and PMA-L-Phe**

	probe/protein			
	PMA-D-Phe/ lysozyme	PMA-L-Phe/ lysozyme	PMA-D-Phe/ BSA	PMA-L-Phe/ BSA
$K_b$ ( $M^{-1}$ )	$2.0 \times 10^6$	$3.3 \times 10^5$	$4.0 \times 10^6$	$3.8 \times 10^5$
$\lambda_{max}$ (nm) absorption	342	342	345	344
$\lambda_{max}$ (nm) fluorescence	377	377	378	378
$\lambda_{max}$ (nm) circular dichroism	(+)-326, (+)-341	(-)-326, (-)-342	(+)-329, (+)-343	(-)-327, (-)-343

in volume during the titration, and no red shifts are noted. While the absorption peak intensities decrease by a small but reproducible amount, on binding to lysozyme, no clear isosbestic points are evident either. These data suggest that the microenvironment of the chromophore in lysozyme is distinct from that in BSA and the environment is polar. The spectral changes observed here are similar to those obtained with PMA-L-Phe/lysozyme, and both probes may reside at the same site on lysozyme.<sup>9</sup>

**Binding Isotherms.** To quantify the binding affinities with the above proteins, the absorption spectral data are used to construct the binding isotherms using the Scatchard equation (Figure 2).<sup>16</sup> Linear fit to the binding isotherm of PMA-D-Phe/BSA indicated a binding constant of  $(4.0 \pm 0.3) \times 10^6 M^{-1}$  (Figure 2A, Table 1) and a binding site size of 2. Note that the binding constant is an order of magnitude greater than that



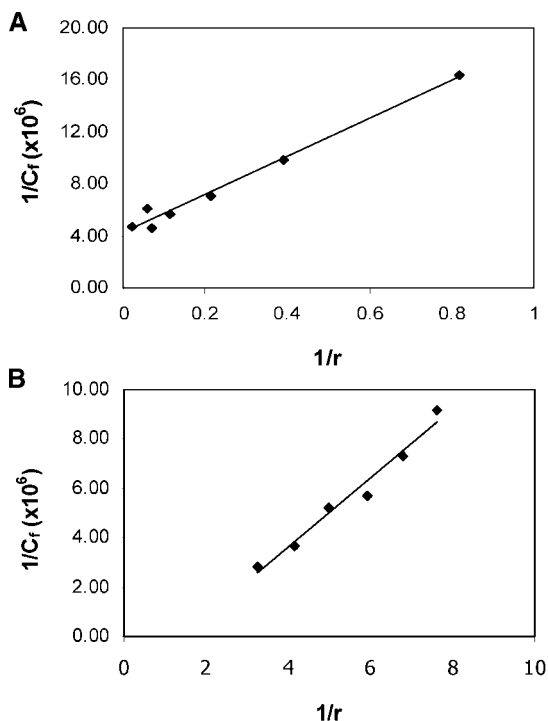


**Figure 2.** (A) The binding isotherm of PMA-D-Phe constructed from the absorption spectral data shown in Figure 1A. The solid line corresponds to the linear fit to the Scatchard equation. (B) The binding isotherm of PMA-D-Phe constructed from the absorption data shown in Figure 1B. The solid line corresponds to the linear fit to the Scatchard equation.

observed with PMA-L-Phe/BSA ( $(3.8 \pm 0.3) \times 10^5 \text{ M}^{-1}$ ) with a chiral selectivity of  $\sim 10$ . Chiral recognition of protein binding sites by Py-Phe enantiomers was also reported with selectivities  $> 100$ . An affinity constant observed with Py-L-Phe/BSA ( $6.7 \times 10^7 \text{ M}^{-1}$ ) is at least 2 orders of magnitude greater than that observed with Py-D-Phe/BSA ( $5.3 \times 10^5 \text{ M}^{-1}$ ).<sup>2</sup>

The selectivity of PMA-Phe for BSA is nearly 10-fold weaker than the corresponding Py-Phe isomers. Even so, these chiral selectivities for the binding of non-natural ligands to a protein are among some of the largest values reported in the literature.<sup>19–21</sup> Since all isomers (PMA-Phe as well as Py-Phe) indicated two binding sites on BSA, the observed selectivities are averages for binding to the two sites. If the two sites have opposite selectivities, then selectivities for the individual sites would be higher than noted here. If one of the two sites has no selectivity or less selectivity, the other site will have a higher selectivity than reported here.

An interesting difference between the PMA-Phe and Py-Phe isomers, in terms of their selectivities for binding to BSA, is that the D-isomer of PMA-Phe is preferred over the L-isomer, while it is the L-isomer of Py-Phe that is preferred over the D-isomer.<sup>2</sup> This selectivity reversal is unexpected, and this provides additional evidence that the chiral center plays an important role in the recognition of the binding site by the pyrenyl probe. The anionic charge of the carboxy terminus of Py-L-Phe is in contrast to the positively charged amino terminus of PMA-L-Phe. In addition to the differences in the charge characteristics, the three-atom linker in PMA-Phe is shorter than the five-atom linker in Py-Phe, and the direction of the peptide bond in PMA-Phe is reversed with respect to that in Py-Phe. The shorter side chain of PMA-Phe is expected to lower the binding constant, and position the chromophore closer to the surface of the protein.

Similar analysis of the binding isotherms of PMA-D-Phe/lysozyme by the Scatchard equation indicated a linear plot (Figure 2B, Table 1). The best fit to the data indicated a binding constant of  $(2.0 \pm 0.1) \times 10^6 \text{ M}^{-1}$ , and a binding site size of 1. This affinity constant is 6-fold greater than the binding affinity of PMA-L-Phe for lysozyme, under similar conditions of pH and ionic strength. The selectivity of the PMA-Phe isomers for binding to lysozyme is significantly larger than the 2-fold selectivity noted with Py-Phe isomers. Note that the D-isomer is preferred over the L-isomer for binding to lysozyme, and this selectivity reversal is similar to that noted with BSA. Therefore, the reversal may be characteristic of the number of intervening atoms between the chiral center and the pyrenyl group. The photocleavage data presented below shows that all four probes cleave at the same site and that cleavage occurs near the binding site.

Given the small size of the chiral center in these probes, the degree of selectivity observed is surprising. A large, open binding site is expected to result in lower selectivity, while a smaller, restrictive binding site is expected to be more discriminating. The smaller PMA-Phe isomers indicated lower selectivity with BSA than Py-Phe isomers, while the opposite trend was noted with lysozyme. The chiral selectivities observed here, however, provide strong evidence for the key role of the asymmetric center of the probe in the binding interaction. If binding is totally dominated by the hydrophobic pyrenyl chromophore, then one would have expected little or no discrimination between the two enantiomers.

**Fluorescence Titrations.** The intense fluorescence of the pyrenyl chromophore allowed the investigation of the ligand–protein interactions by fluorescence spectroscopy. The fluorescence of PMA-D-Phe ( $0.28 \mu\text{M}$ ) is enhanced by the addition of BSA ( $0–10 \mu\text{M}$ , Figure 3A), while the spectra are red-shifted by a mere 1 nm. These observations parallel the fluorescence enhancements observed with PMA-L-Phe/BSA,<sup>9</sup> but they are in contrast to the results reported with Py-Phe/BSA. In the case of the latter, the fluorescence from the D-isomer was enhanced, while that of the L-isomer was quenched (Table 2).<sup>1</sup> The fluorescence enhancements noted with Py-D-Phe suggest that residues such as Trp or Tyr, which are known to quench pyrene emission,<sup>22,23</sup> are not present at the probe binding site, or near it. Thus, the microenvironments around the PMA-Phe probes in BSA differ significantly from those of Py-L-Phe isomers, and this conclusion is also supported by the photocleavage results described later.

In contrast to the fluorescence data obtained with BSA, the titration of PMA-D-Phe ( $0.7 \mu\text{M}$ ) with increasing concentrations of lysozyme ( $0, 2, 4, 6, 8$ , and  $10 \mu\text{M}$ ) indicated weak quenching of the pyrenyl fluorescence (Figure 3B). The data were corrected for the decrease in absorbance at the excitation wavelength. No peak shifts or excimer/excimer emission are observed, and these results are similar to those observed with PMA-L-Phe or Py-Phe isomers.

**Fluorescence Quenching Studies.** The degree of access of the probe to the aqueous phase can be estimated in fluorescence quenching studies. For example, probes that are buried deeply in the protein will be protected from quenchers present in the aqueous phase, while probes that are bound on the surface of the protein will be less protected or exposed.<sup>6</sup> For the current studies, hexamine cobalt(III) chloride (CoHA) was selected as the fluorescence quencher. This is because (1) CoHA quenches pyrenyl fluorescence at diffusion controlled rate constants, (2) CoHA is highly soluble in aqueous media so that suitable concentrations of the quencher can be used in the

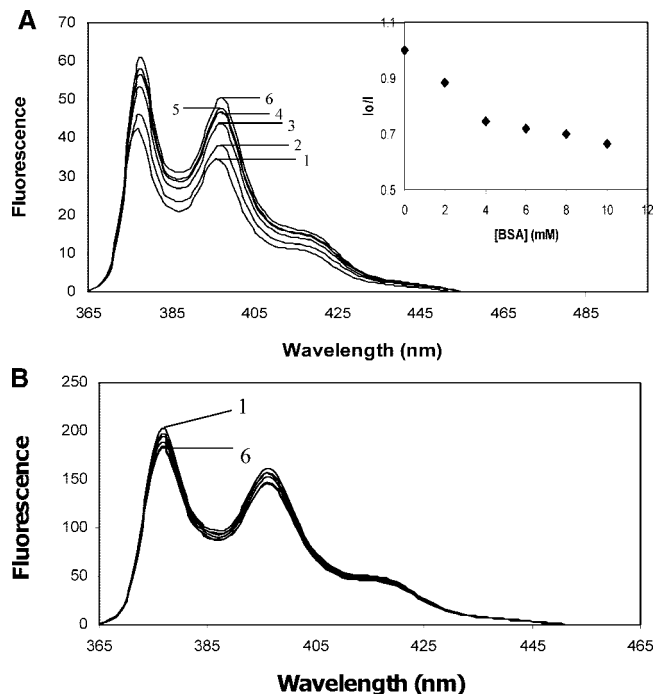


**Figure 3.** (A) Fluorescence spectra of PMA-D-Phe (0.28  $\mu\text{M}$ ) recorded in the presence of increasing concentrations of BSA (0–10  $\mu\text{M}$ ): (1) 0  $\mu\text{M}$ , (2) 2  $\mu\text{M}$ , (3) 4  $\mu\text{M}$ , (4) 6  $\mu\text{M}$ , (5) 8  $\mu\text{M}$ , and (6) 10  $\mu\text{M}$ . The excitation wavelength was at the isosbestic point, 344 nm. The inset shows the plot of normalized intensity ( $I_0/I$ ) vs BSA concentration. (B) The fluorescence spectra of PMA-D-Phe (0.7  $\mu\text{M}$ ) recorded in the presence of increasing concentrations of lysozyme (0–10  $\mu\text{M}$ ): (1) 0  $\mu\text{M}$ , (2) 2  $\mu\text{M}$ , (3) 4  $\mu\text{M}$ , (4) 6  $\mu\text{M}$ , (5) 8  $\mu\text{M}$ , and (6) 10  $\mu\text{M}$ . The excitation wavelength was at 344 nm.

**TABLE 2: Quenching of Probe Fluorescence by Proteins**

enantiomer	probe + lysozyme	probe + BSA
PMA-D-Phe	weak quenching ( $K_{sv} = 0.011 \times 10^3 \text{ M}^{-1}$ )	intensity enhancing
PMA-L-Phe	weak quenching (no data)	intensity enhancing
Py-D-Phe	weak quenching (no data)	intensity enhancing
Py-L-Phe	weak quenching (no data)	quenching (exciplex emission) ( $K_{sv} = 4.57 \times 10^5 \text{ M}^{-1}$ )

studies, (3) CoHA is not fluorescent, (4) CoHA has only weak affinity for most proteins, and (5) CoHA is used to induce protein cleavage with pyrenyl probes. Quenching of the pyrenyl excited states by CoHA generates radical intermediates, which are capable of cleaving the peptide backbone.<sup>10</sup> Feasibility of the photocleavage studies, which are described later, directly depends on the accessibility of the chromophore to CoHA. Hence, the quenching constants with CoHA are expected to be useful indicators for the success of the photocleavage studies. In addition, comparing the quenching constants of the two enantiomers will be useful to differentiate further between their binding environments or their access to the aqueous phase.

The probe–protein mixtures were titrated with CoHA, and the fluorescence intensities have been monitored at 378 nm for PMA-Phe/BSA or 377 nm for PMA-Phe/lysozyme (excitation at 344 nm). Quenching constants ( $K_{sv}$ ) were obtained from eq 2,<sup>24</sup> where  $I_0$  is the fluorescence intensity in the absence of the quencher and  $I$  is the intensity in the presence of the quencher.

$$I_0/I = 1 + K_{sv}[\text{CoHA}] \quad (2)$$

The quenching constants obtained from these data are collected in Table 3, and probes bound to the protein are quenched with lower  $K_{sv}$  values than the free probes. Assuming that the fluorescence lifetimes of the probes are similar, the quenching constants can provide a rough estimate of the degree of accessibility of the bound probes. CoHA quenches emission of PMA-D-Phe (0.7  $\mu\text{M}$ ) bound to BSA (10  $\mu\text{M}$ ) ( $K_{sv} = 0.15 \times 10^3 \text{ M}^{-1}$ ), while the addition of the quencher to PMA-L-Phe (0.7  $\mu\text{M}$ ) bound to BSA (10  $\mu\text{M}$ ) enhances the emission (Table 3) which is interesting.

Emission enhancements are very likely due to changes in the microenvironment around the chromophore embedded in the protein matrix. The increase of PMA-Phe fluorescence intensity was also observed when PMA-Phe was dissolved in methanol. These could be due to increased rigidity, change in local polarity, or movement of a residue out of the binding pocket which serves as a quencher. This contrasting difference between the two enantiomers further supports the notion that the probe environments are distinct in some respects, which in turn is responsible for the observed chiral selectivity.

In the case of lysozyme (10  $\mu\text{M}$ ), the quenching constants of the D- and L-isomers of PMA-Phe differed by only a small percent ( $0.72 \times 10^3$  and  $0.79 \times 10^3 \text{ M}^{-1}$ , respectively). Both enantiomers are accessible to CoHA, and also protected by the protein matrix to a considerable extent. The above quenching data, on the whole, indicate the close association of the pyrenyl chromophores of the probes with the chiral amino acid residues of the protein. Such association is expected to alter the chiral environment of the chromophore and change the CD bands of the probes, and these data are presented below.

**Circular Dichroism Spectra.** The CD spectra of the PMA-Phe enantiomers, in the absence of the protein, indicated a mirror image relationship (300–400 nm, Figure 4A). These spectra show that the chiral center provides an asymmetric environment for the electronic transitions of the pyrenyl chromophore. Note that the proteins themselves do not have CD bands in this region (300–400 nm), and the CD spectra provide a fingerprint of the environment surrounding the probe. Addition of BSA (50  $\mu\text{M}$ ) to a solution of PMA-D-Phe (30  $\mu\text{M}$ ) resulted in a large decrease in the intensity of the major CD peaks (320–360 nm, Figure 4B). These decreases are in contrast to the large intensity increases and a small red shift (1 nm) noted with PMA-L-Phe/BSA (Figure 4B). The CD spectral changes clearly indicate that the pyrenyl chromophore behaves differently depending on its protein environment, and the chromophore is in close association with the asymmetric residues of the protein. The CD spectra of the pyrenyl probe provide a characteristic signature of its chiral environment.

In contrast to the changes with BSA, the CD spectra of PMA-D-Phe (30  $\mu\text{M}$ ) and PMA-L-Phe (30  $\mu\text{M}$ ) recorded in the presence of lysozyme (50  $\mu\text{M}$ ) indicated only modest changes. In the case of the D-enantiomer, there was a significant decrease

**TABLE 3: Stern–Volmer Constants ( $K_{sv}$ ) for the Quenching of Probe Fluorescence by Hexammine Cobalt(III) Chloride**

enantiomer	free probe ( $\text{M}^{-1}$ )	probe + lysozyme ( $\text{M}^{-1}$ )	probe + BSA ( $\text{M}^{-1}$ )
PMA-D-Phe	$2.31 \times 10^3$	$0.72 \times 10^3$	$0.15 \times 10^3$
PMA-L-Phe	$1.28 \times 10^3$	$0.79 \times 10^3$	intensity enhanced
Py-D-Phe	$1.9 \times 10^3$	$0.53 \times 10^3$	intensity enhanced
Py-L-Phe	$1.9 \times 10^3$	$1.4 \times 10^3$	$0.247 \times 10^3$

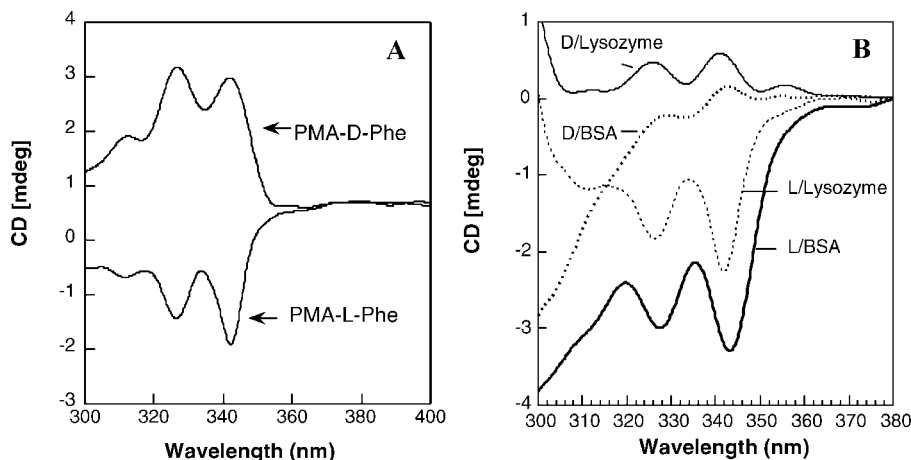


**Figure 4.** The CD spectra of PMA-D-Phe (30  $\mu$ M) and PMA-L-Phe (30  $\mu$ M) in Tris buffer as free probes (A) and bound (B) to BSA (50  $\mu$ M) or lysozyme (50  $\mu$ M), as marked.

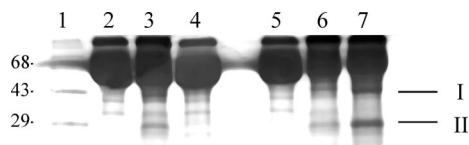


**Figure 5.** SDS-PAGE of the photocleavage products of BSA by the PMA-Phe enantiomers. Lane 1 contained mol. wt. markers, shown in kDa. Lanes 2 and 3 contained BSA (15  $\mu$ M), PMA-D-Phe (15  $\mu$ M), and CoHA (1 mM), and lane 4 contained BSA (15  $\mu$ M) and PMA-D-Phe (15  $\mu$ M). While lane 2 is the dark control, samples in lanes 3 and 4 were exposed to 342 nm radiation (20 min). Lanes 5 and 6 contained a mixture of BSA (15  $\mu$ M), PMA-L-Phe (15  $\mu$ M), and CoHA (1 mM). Lane 5 is the dark control, while the sample in lane 6 was exposed to 342 nm radiation for 20 min. Lane 7 contained BSA (15  $\mu$ M), Py-L-Phe (15  $\mu$ M), and CoHA (1 mM) which was irradiated at 342 nm for 20 min.

in intensities but changes with the L-enantiomer have been marginal. Thus, the two proteins interact with these probes in a substantially different manner and two isomers differ considerably in terms of their asymmetric environment.

Perhaps, the binding site in BSA is more restrictive, interacts more strongly with the probe, or restricts the number of conformations that the probe can achieve at the binding site. Unrestricted rotation of the pyrenyl chromophore around one of the linker bonds, for example, is expected to result in no CD signal at all. In contrast, the weaker CD signals and low chiral selectivity noted with lysozyme suggest that its binding site is more accommodative, less restrictive, and perhaps allows for greater flexibility. It is intriguing to note that the observed chiral selectivity and the extent of changes produced in the intensities of the CD bands of the probes have a strong correlation. The relationship between these binding features and the photoreactivities of the enantiomers is investigated in protein cleavage studies.

**Protein Photocleavage Studies.** An important detail needed for the adequate description of the binding of a ligand to the protein is the identity of its binding site. The binding sites of ligands, which are capable of cleaving the protein, can be ascertained by identifying their corresponding cleavage sites on the protein. Earlier studies showed that the pyrenyl chromophore (Py) by itself does not cleave proteins but the cation radical derived from the Py excited state induces protein fragmentation.

Irradiation of a mixture of BSA (15  $\mu$ M), PMA-D-Phe (15  $\mu$ M), and CoHA (1 mM) at 342 nm resulted in two photocleavage fragments of mol. wt.  $\sim$ 40 000 and  $\sim$ 28 000 (Figure 5, lanes 3 and 6). The molecular masses of the two fragments (I and II)

roughly add up to that of BSA, and cleavage perhaps occurs at a single site or a few residues apart. The yields of the fragments are less than 5%, which is much lower than that observed with Py-Phe/BSA (lane 7, 21%). Note that addition of CoHA increased the probe fluorescence, and hence, the production of the reactive radical intermediates is significantly less. No photocleavage occurred in the absence of CoHA (lane 4), without the probe (data not shown), or when the reaction mixture was left in the dark (lanes 2 and 5). Both PMA-D-Phe and PMA-L-Phe seem to cleave BSA at the same site (lanes 3 and 6), despite the 10-fold chiral selectivity noted for the binding.

The photocleavage fragments from the BSA/PMA-Phe reaction mixture correspond with the product bands observed with BSA/Py-Phe (Figure 5, lane 7), but the latter probe produced greater yield. The low yield with PMA-Phe isomers could be due to its shorter linker. The radical intermediate generated at the pyrenyl chromophore is perhaps a few angstroms away from the reactive site which can result in reduced yields. The opposite charge on the PMA-Phe isomers could be another important reason, and the cleavage site is closer to a positively charged residue and negative charge on the probe would facilitate the photocleavage.

The above photocleavage data clearly show that the length of the linker and/or the charge on the probe play a critical role in controlling the photoreactivity of the probes. These possibilities will be distinguished in future studies where the charge reversal and linker length will be varied systematically. Sequencing of the products from the BSA/PMA-Phe reaction was not attempted due to the low yields, but these products qualitatively match with those of Py-Phe.

Photocleavage studies with lysozyme, on the other hand, are very encouraging. Irradiation of a mixture of PMA-D-Phe (15  $\mu$ M), lysozyme (15  $\mu$ M), and CoHA (1 mM) at 342 nm resulted in the facile cleavage of the protein, in high yields (52%, Figure 6). Photocleavage of lysozyme resulted in two fragments of molecular weights 11 and 3 kDa (bands I and II, lane 3). No products are produced in the absence of light (lane 2), without CoHA (lane 6), or in the absence of PMA-D-Phe (data not shown). The probe, CoHA, and light, therefore, are essential for protein photocleavage. The photofragments of lysozyme observed with PMA-D-Phe (lane 3) matched with those obtained with PMA-L-Phe (lane 5).

Despite the differences in the binding constants of the two enantiomers, their photocleavage yields are nearly the same (Table 4). The photocleavage yields of PMA-L-Phe isomers



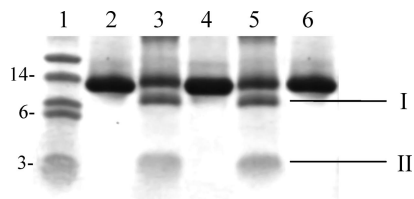


**Figure 6.** SDS-PAGE of lysozyme photoproducts observed with PMA-Phe enantiomers. Lane 1 contained mol. wt. markers, shown in kDa. Lanes 2 and 3 contained a mixture of lysozyme (15  $\mu$ M), PMA-D-Phe (15  $\mu$ M), and CoHA (1 mM), and lanes 4 and 5 contained a mixture of lysozyme (15  $\mu$ M), PMA-L-Phe (15  $\mu$ M), and CoHA (1 mM). Lanes 2 and 4 are the dark controls, while the samples in lanes 3 and 5 were exposed to 342 nm radiation for 10 min. Lane 6 contained lysozyme (15  $\mu$ M) and PMA-D-Phe (15  $\mu$ M), which was exposed to 342 nm radiation for 10 min.

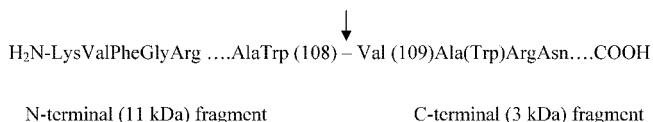
**TABLE 4: Yields of Lysozyme Photocleavage**

probe	[CoHA]	% Fl. quenching <sup>a</sup>	% photochemical yield
PMA-D-Phe	1 mM	42	52
PMA-L-Phe	1 mM	44	57
Py-D-Phe	1 mM	35	21
Py-L-Phe	1 mM	58	35

<sup>a</sup> Calculated using the formula  $100 - (100/(1 + K_{sv} [1 \text{ mM}]))$ .

## CHART 2: Identity of the Primary Photocleavage Site on Lysozyme

PMA-D/L-Phe cleavage site on lysozyme:

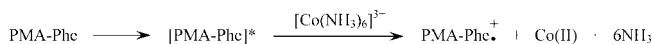


(57%) are the highest reported thus far, and they are substantially larger than the 35% yield reported for Py-L-Phe, under similar conditions of irradiation. This improvement in the yield is to be attributed to the more facile access of the pyrenyl chromophore to CoHA.

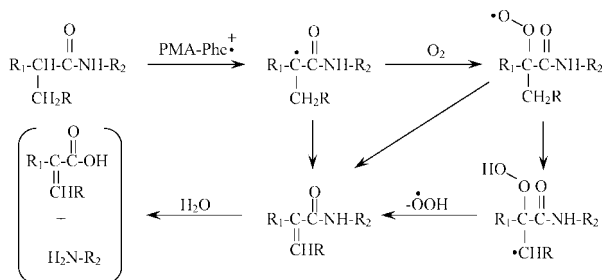
Another powerful trend is clear with the photocleavage data. Since the PMA-Phe enantiomers show a strong discrimination but give essentially the same yields and cleavage patterns, it is concluded that the binding site and the cleavage site differ to a significant extent. It is possible that not all residues at the binding site are amenable to photocleavage chemistry, and only selected amino acid residues are appropriately oriented for the chemistry to occur. For example, access to a suitable H-atom for abstraction (Trp-108) may be necessary to initiate the cleavage. Some exploration of the surroundings by the bound probe may be necessary for the cleavage to occur.

**Amino Acid Sequencing Studies.** The photocleavage site and, hence, the probable binding site of the probe on the protein are assessed by sequencing the photofragments. Thus, N-terminal sequencing of the 11 kDa fragment from PMA-D-Phe/lysozyme reaction indicated residues KVFGK, which are the known N-terminal residues of lysozyme. The newly formed N-terminus of the 3 kDa fragment was sequenceable, and this analysis indicated residues VA(W)RN, where W was modified in some way and undetectable in the HPLC analysis. From the known amino acid sequence of lysozyme and the above sequencing data, it is clear that lysozyme is cleaved between residues Trp108-Val109 (Chart 2). The 11 kDa band, therefore, arises from the N-terminus of lysozyme, and the 3 kDa band is the C-terminal fragment. Despite all the differences in the photophysical data and the binding affinities, both PMA-Phe

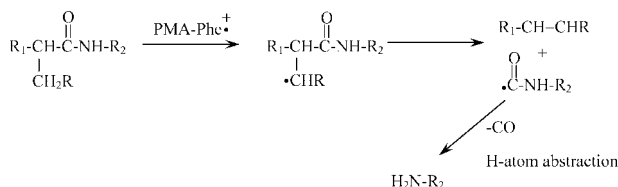
## SCHEME 1: Possible Mechanisms for Lysozyme Photocleavage



### $\alpha$ -Hydrogen abstraction



### $\beta$ -Hydrogen abstraction



enantiomers and the Py-Phe enantiomers cleave lysozyme at the same location. This consistency is perhaps due to the fact that the large, hydrophobic binding site on lysozyme is located at the so-called hinge region. All four probes bind at this site, albeit with differing affinities.

A secondary cleavage site was observed with PMA-Phe enantiomers, in addition to the above cleavage site. The 3 kDa band from PMA-D-Phe enantiomers also indicated a minor product (<5%) whose N-terminus indicated residues KVFGK. Therefore, this is a 3 kDa N-terminal fragment, which coeluted with the C-terminal fragment. The corresponding 11 kDa C-terminal fragment is not detectable in our sequencing studies because its N-terminus is perhaps not amenable to the sequencing chemistry. The second cleavage site is therefore estimated to be somewhere between residues 19–23. Therefore, photocleavage by PMA-D-Phe is highly selective (52:5, the relative yields of the two fragments) but not specific to one site. However, this minor product was not observed with the L-isomer or with the Py-Phe isomers. Thus, there are subtle differences between these probes.

It is noteworthy that both Py-L-Phe and Py-D-Phe cleave lysozyme at a single site, site specifically, and the above minor product was not observed with these probes. This loss of specificity with PMA-Phe, but high selectivity and enhanced cleavage yield, clearly indicate the strong role of the probe structural features on the protein photocleavage. The improved photocleavage yields with PMA-Phe are a welcome change for photocleavage applications.

**Photoreaction Quenching Studies.** Flash photolysis studies with Py-Phe indicated that the protein photocleavage by pyrenyl probes proceeds via the formation of pyrene-derived cation radical.<sup>3</sup> A similar pathway is anticipated with PMA-Phe, and hence, quenching of this cation radical intermediate is expected to inhibit the photoreaction (Scheme 1).

Addition of ethanolamine to the reaction mixture (>20 mM) resulted in a significant inhibition of the photoreaction (Figure 7). Note that the addition of 8 mM ethanolamine was adequate to quench the photoreaction of Py-Phe almost completely ( $K_{sv} = 60 \text{ M}^{-1}$ ).<sup>2</sup> Therefore, the reactive intermediates involved in the PMA-Phe reaction are also intercepted by this quencher to

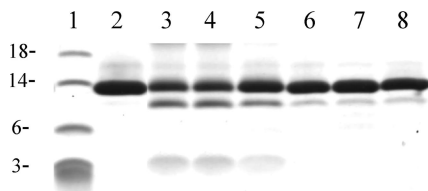


**Figure 7.** Inhibition of the photocleavage of lysozyme by ethanolamine (10–50 mM). Lane 1 contained mol. wt. markers, shown in kDa. Lanes 2 and 3 contained a mixture of lysozyme (15  $\mu$ M), PMA-L-Phe (15  $\mu$ M), and CoHA (1 mM). Lanes 4–8 contained lysozyme (15  $\mu$ M), PMA-L-Phe (15  $\mu$ M), CoHA (1 mM), and ethanolamine (10, 20, 30, 40, and 50 mM, respectively). Lane 2 is the dark control, while the samples in lanes 3–8 were exposed to 342 nm radiation (10 min).

a considerable extent. The decrease in sensitivity to ethanolamine could be due to a shorter lifetime of the cation radical derived from PMA-Phe/lysozyme complex. This shortening of the lifetime of the cation could be due to enhanced reactivity, resulting in improved photocleavage yields, which is consistent with the much higher yield of lysozyme photocleavage by PMA-Phe than by Py-Phe.

As proposed earlier, H-atom abstraction from the side chains of the amino acid residues present at the probe binding site might be responsible for the photocleavage. Two distinct pathways ( $\alpha$ - or  $\beta$ -hydrogen abstraction) are shown in Scheme 1. Note that  $\alpha$ -hydrogen abstraction is likely to result in cleavage on the C-terminal side of the residue and a sequeable N-terminus (as seen here). On the other hand,  $\beta$ -hydrogen abstraction is likely to produce cleavage on the N-terminal side of the residue and also a sequeable N-terminus. Other pathways proposed for radical-induced protein cleavage (not shown here) do not generate a free amino terminus. Therefore, H-atom abstraction from the Trp residue but not from Val is likely responsible for cleavage at Trp108-Val109.

Molecular modeling of lysozyme, using its crystal structure<sup>25</sup> (Supporting Information), shows that the side chains of Trp108 and Val109 are exposed into the active site cavity. If the pyrenyl probes bind at this site with their hydrophobic chromophore partially buried at this site, then H-atom abstraction from Trp108 could result in the observed cleavage.

The enantiomeric selectivities for the binding of PMA-Phe and Py-Phe enantiomers differ substantially, but the major cleavage site is common. We conclude that the binding site and the reactive site differ to some extent, but they are within close proximity. Since the reactive intermediates that are responsible for the photocleavage are short-lived, and the photocleavage is highly selective, these sites can not be too far apart. This distinction between the binding site and the reactive site is important in the design of future studies.

**Acknowledgment.** C.V.K. thanks the NSF (DMR-0300631, DMR-0604815). A.B. thanks Srinakharinwirot University Research Fund (SWURF) and Thailand Research Fund (TRF) under senior research fellow grant of Professor M. R. Jisnusun Svasti. This publication is in celebration of the 70th Birth year of Professor Nicholas J. Turro.

**Supporting Information Available:** The three-dimensional structure of lysozyme backbone, looking down the substrate binding cavity, is shown here. The major cleavage site of lysozyme was found to be between Trp108-Val109. The  $\alpha$ -hydrogen of Trp108 and the side chain of Val109 (not shown) are readily accessible to ligands bound in the active site. This information is available free of charge via the Internet at <http://pubs.acs.org>.

## References and Notes

- (1) Kumar, C. V.; Buranaprapuk, A. *Angew. Chem., Int. Ed. Engl.* **1997**, 36, 2085.
- (2) Kumar, C. V.; Buranaprapuk, A.; Sze, H. C.; Jockusch, S.; Turro, N. J. *Proc. Natl. Acad. Sci. U.S.A.* **2002**, 99, 5810.
- (3) Kumar, C. V.; Tolosa, L. M. *J. Phys. Chem.* **1993**, 97, 13914.
- (4) Kumar, C. V.; Tolosa, L. M. *Indian J. Chem.* **1999**, 38B, 1170.
- (5) Kumar, C. V.; Buranaprapuk, A. *J. Am. Chem. Soc.* **1999**, 121, 4262.
- (6) Buranaprapuk, A.; Kumar, C. V.; Jockusch, S.; Turro, N. J. *Tetrahedron* **2000**, 56, 7019.
- (7) Kumar, C. V.; Buranaprapuk, A.; Sze, H. C. *Chem. Commun.* **2001**, 297.
- (8) Kumar, C. V.; Buranaprapuk, A.; Thota, J. *Proc. Indian Acad. Sci. (Chem. Sci.)* **2002**, 114, 539.
- (9) Buranaprapuk, A.; Chaivisuthangkura, P.; Svasti, J.; Kumar, C. V. *Lett. Org. Chem.* **2005**, 2, 554.
- (10) Kumar, C. V.; Buranaprapuk, A.; Opiteck, G. J.; Moyer, M. B.; Jockusch, S.; Turro, N. J. *Proc. Natl. Acad. Sci. U.S.A.* **1998**, 95, 10361.
- (11) Chaudhari, A.; Kumar, C. V. *Microporous Mesoporous Mater.* **2005**, 77, 175.
- (12) Nelson, G.; Warner, I. M. *J. Phys. Chem.* **1990**, 94, 576.
- (13) Baliah, V.; Pillay, M. K. *Indian J. Chem.* **1971**, 9, 815.
- (14) Kumar, C. V. In *Photoprocesses in Organized Media*; Ramamurthy, V., Ed.; VCH Publishers: New York, 1991; pp 783–816.
- (15) Cantor, C. R.; Schimmel, P. R. In *Biophysical Chemistry, Part I*; W. H. Freeman: San Francisco, CA, 1980; p 49.
- (16) Scatchard, G. *Ann. N.Y. Acad. Sci.* **1949**, 51, 660.
- (17) Schagger, H.; von Jagow, G. *Anal. Biochem.* **1987**, 166, 368.
- (18) Winnik, F. M. *Chem. Rev.* **1993**, 93, 587.
- (19) Allenmark, S.; Andersson, S. *Chirality* **1992**, 4, 24.
- (20) Cserhati, T.; Forgacs, E. *Int. J. Bio-Chromatogr.* **1999**, 4, 203.
- (21) Taura, T. *Inorg. Chim. Acta* **1996**, 252, 1.
- (22) Palmans, J. P.; Van der Auweraer, M.; Swinner, A. M.; De Schryver, F. C. *J. Am. Chem. Soc.* **1984**, 106, 7721.
- (23) Vekshin, N. L. *Anal. Chim. Acta* **1989**, 227, 267.
- (24) Kumar, C. V.; Barton, J. K.; Turro, N. J. *J. Am. Chem. Soc.* **1985**, 107, 5518.
- (25) Diamond, R.; Phillips, D. C.; Blake, C. C. F.; North, A. C. T. *J. Mol. Biol.* **1974**, 82, 371.

JP802791C